AFRL-RZ-WP-TP-2012-0090

FLUX PINNING EFFECTS OF Y_2O_3 NANOPARTICULATE DISPERSIONS IN MULTILAYERED YBCO THIN FILMS (POSTPRINT)

T.A. Campbell, T.J. Haugan, and P.N. Barnes

Mechanical Energy Conversion Branch
Energy/Power/Thermal Division

I. Maartense, J. Murphy, and L. Brunke

University of Dayton Research Institute

FEBRUARY 2012

AIR FORCE RESEARCH LABORATORY
PROPULSION DIRECTORATE
WRIGHT-PATTERSON AIR FORCE BASE, OH 45433-7251
AIR FORCE MATERIEL COMMAND
UNITED STATES AIR FORCE

REPORT DOCUMENTATION PAGE

Form Approved
OMB No. 0704-0188

1. REPORT DATE *(DD-MM-YY)*	2. REPORT TYPE	3. DATES COVERED *(From - To)*
February 2012	Journal Article Postprint	01 January 2003 – 01 January 2005

4. TITLE AND SUBTITLE

FLUX PINNING EFFECTS OF Y_2O_3 NANOPARTICULATE DISPERSIONS IN MULTILAYERED YBCO THIN FILMS (POSTPRINT)

5a. CONTRACT NUMBER
In-house

5b. GRANT NUMBER

5c. PROGRAM ELEMENT NUMBER
62203F

6. AUTHOR(S)

T.A. Campbell, T.J. Haugan, and P.N. Barnes (AFRL/RZPG)
I. Maartense, J. Murphy, and L. Brunke (University of Dayton Research Institute)

5d. PROJECT NUMBER
3145

5e. TASK NUMBER
32

5f. WORK UNIT NUMBER
314532Z9

7. PERFORMING ORGANIZATION NAME(S) AND ADDRESS(ES)

Mechanical Energy Conversion Branch (AFRL/RZPG)
Energy/Power/Thermal Division
Air Force Research Laboratory, Propulsion Directorate
Wright-Patterson Air Force Base, OH 45433-7251
Air Force Materiel Command, United States Air Force

University of Dayton Research Institute
Dayton, OH

8. PERFORMING ORGANIZATION REPORT NUMBER
AFRL-RZ-WP-TP-2012-0090

9. SPONSORING/MONITORING AGENCY NAME(S) AND ADDRESS(ES)

Air Force Research Laboratory
Propulsion Directorate
Wright-Patterson Air Force Base, OH 45433-7251
Air Force Materiel Command
United States Air Force

10. SPONSORING/MONITORING AGENCY ACRONYM(S)
AFRL/RZPG

11. SPONSORING/MONITORING AGENCY REPORT NUMBER(S)
AFRL-RZ-WP-TP-2012-0090

12. DISTRIBUTION/AVAILABILITY STATEMENT

Approved for public release; distribution unlimited.

13. SUPPLEMENTARY NOTES

Journal article published in *Physica C*, Vol. 423, 2005. Work on this effort was completed in 2005.

PA Case Number: AFRL/WS-05-0754; Clearance Date: 06 Dec 2005.

14. ABSTRACT

The flux pinning effects of Y_2O_3 nanoparticulate inclusions in $YBa_2Cu_3O_{7-\delta}$ (Y123 or YBCO) thin films using $(Y_2O_3/Y123) \times N$ multilayer structures were studied. The multilayer films were made with pulsed laser deposition (PLD) on $SrTiO_3$ and $LaAlO_3$ substrates with a Y_2O_3 nanoparticulate pseudo-layer thickness ranging from 0.2 to 1.4 nm, and YBCO layer thickness varying from 7 to 50 nm. Scanning electron microscopy images showed well-defined nanoparticle formation on film surfaces, with an approximate number density of $(0.8–1.6) \times 10^{11}$ particles/cm^2 depending on Y_2O_3 thickness. Minor reductions in the critical temperature (T_c) were measured for each increase in Y_2O_3 pseudo-layer thickness. Transport critical currents (77 K, self-field) of 3–5 MA/cm^2 were consistently achieved for composite films with ≤ 0.6 nm Y_2O_3 pseudo-layer thicknesses. Magnetic J_c measurements using vibrating sample magnetometry ($H \leq 9$ T, @70 and 77 K) showed a degradation of film properties for Y_2O_3 pseudo-layer thickness greater than 0.6 nm. A comparison to Y211/Y123 multilayer films showed the thinner Y_2O_3 pseudo-layer films exhibited similar properties.

15. SUBJECT TERMS

flux pinning, density, magnetometry, transport, nanoparticle, images, microscopy, nanoparticulate, pulsed laser deposition

16. SECURITY CLASSIFICATION OF:			17. LIMITATION OF ABSTRACT:	18. NUMBER OF PAGES	19a. NAME OF RESPONSIBLE PERSON (Monitor)
a. REPORT	b. ABSTRACT	c. THIS PAGE			Timothy J. Haugan
Unclassified	Unclassified	Unclassified	SAR	14	19b. TELEPHONE NUMBER *(Include Area Code)* N/A

Available online at www.sciencedirect.com
SCIENCE DIRECT®
Physica C 423 (2005) 1–8
PHYSICA C
www.elsevier.com/locate/physc

Flux pinning effects of Y_2O_3 nanoparticulate dispersions in multilayered YBCO thin films

T.A. Campbell [a], T.J. Haugan [a], I. Maartense [b], J. Murphy [b], L. Brunke [b], P.N. Barnes [a,*]

[a] *Air Force Research Laboratory, Propulsion Directorate, AFRL/PRPG, 1950 Fifth Street, Building 450, Wright-Patterson AFB, OH 45433, USA*

[b] *University of Dayton Research Institute, Dayton, OH, USA*

Received 23 July 2004; received in revised form 19 September 2004; accepted 22 September 2004
Available online 22 April 2005

Abstract

The flux pinning effects of Y_2O_3 nanoparticulate inclusions in $YBa_2Cu_3O_{7-\delta}$ (Y123 or YBCO) thin films using $(Y_2O_3/Y123) \times N$ multilayer structures were studied. The multilayer films were made with pulsed laser deposition (PLD) on $SrTiO_3$ and $LaAlO_3$ substrates with a Y_2O_3 nanoparticulate 'pseudo-layer' thickness ranging from 0.2 to 1.4 nm, and YBCO layer thickness varying from 7 to 50 nm. Scanning electron microscopy images showed well-defined nanoparticle formation on film surfaces, with an approximate number density of $(0.8–1.6) \times 10^{11}$ particles/cm^2 depending on Y_2O_3 thickness. Minor reductions in the critical temperature (T_c) were measured for each increase in Y_2O_3 pseudo-layer thickness. Transport critical currents (77 K, self-field) of 3–5 MA/cm^2 were consistently achieved for composite films with $\leqslant$0.6 nm Y_2O_3 pseudo-layer thicknesses. Magnetic J_c measurements using vibrating sample magnetometry ($H \leqslant 9$ T, @70 and 77 K) showed a degradation of film properties for Y_2O_3 pseudo-layer thickness greater than 0.6 nm. A comparison to Y211/Y123 multilayer films showed the thinner Y_2O_3 pseudo-layer films exhibited similar properties.
Published by Elsevier B.V.

PACS: 74.60; 74.60.G; 74.60.J; 74.62

Keywords: Flux pinning; Yttrium oxide (Y_2O_3); Multilayers; Critical current density

1. Introduction

The improvement of the critical current density (J_c) in high temperature superconducting (HTS)

* Corresponding author. Tel.: +1 937 255 4410; fax: +1 937 656 4095.
E-mail address: paul.barnes@wpafb.af.mil (P.N. Barnes).

0921-4534/$ - see front matter Published by Elsevier B.V.
doi:10.1016/j.physc.2004.09.018

$YBa_2Cu_3O_{7-\delta}$ (Y123 or YBCO) coated conductors in applied magnetic fields is needed to reduce the weight and costs of cryogenic power devices such as HTS generators and motors [1]. It is also important for $J_c(H)$ to reach values of 10^6 A/cm^2 in applied field strengths of a few Tesla at 65–77 K [2]. The increase in J_c is typically accomplished through the use of magnetic flux pinning in the HTS material [3–13]. One means of accomplishing this is the incorporation of non-superconducting particles into YBCO, such as Y_2O_3. The flux-pinning properties of Y_2O_3 in YBCO thin films have previously been reported in films prepared by sputtering and metallorganic vapor deposition (MOCVD) [5–7]. Films with additions of Y_2O_3 that were prepared by MOCVD did show some improved $J_c(H)$ values [6].

There are several reasons for considering Y_2O_3 inclusions for magnetic flux pinning using the multilayered nanoparticulate dispersion approach. A close lattice mismatch between YBCO and Y_2O_3 of $\sim$0.6% exists which should reduce the intrinsic strain of the composite material. Also, Y_2O_3 is known to deposit epitaxially with YBCO [14], avoiding any non-optimized growth that may occur at the interfaces of the two materials. Y_2O_3 has a simple cubic structure which should be easier to deposit epitaxially compared to the more complex structure of Y211. It should be noted, however, that the closer lattice mismatch can change the shape of the nanoparticle inclusions. Such differences may result in potentially improved $J_c(H)$ performance by reducing current blocking while also maintaining pinning properties. The addition of Y_2O_3 nanoparticles is potentially complicated by phase equilibrium studies that indicate Y_2O_3 and Y123 react to form Y_2BaCuO_5 (Y211) phase additions. However, both Y_2O_3 and Y211 have been observed to form in metastable thin films depending on the processing conditions and volume fraction additions [5,7].

This paper considers the introduction of Y_2O_3 nanoparticulate inclusions into YBCO coated conductors using a $(Y_2O_3/Y123) \times N$ multilayer structure. Previously, Y211 nanoparticle inclusions were considered in a $(Y211/Y123) \times N$ multilayer superlattice type structure, which significantly enhanced the $J_c(H)$ properties of the YBCO+ nanoparticle films [3]. The $(Y211/Y123) \times N$ structure produced a near uniform inclusion of Y211 nanoparticles averaging 8 nm in diameter, in a superlattice type structure where the individual layers of Y211 particles were separated by well-defined Y123 layers. It is expected that similar structures can be obtained by using Y_2O_3 additions, however differences of pinning might be expected because of variances of nanoparticle shapes and number densities.

2. Experimental

The Y_2O_3 and Y123 multi-layer films were grown by pulsed laser deposition using the same basic conditions as reported for Y211/Y123 multi-layer thin films [3,15]. The depositions were done using an excimer laser (Lambda Physik USA, model LPX 305i) operating at a 248 nm wavelength (KrF). The laser fluence was approximately 3.2 J/cm^2 for the Y123 layers and 1.3 J/cm^2 for the Y_2O_3 pseudo-layers, with an ablation spot size of 1 mm $\times$ 6.5 mm. The reduction in energy during the Y_2O_3 deposition was accomplished by repeatedly sliding an attenuating mirror into the beam path prior to the Y_2O_3 target rotating into position and then back out of the path as the Y123 target rotated into position.

In this work, the thickness of the Y_2O_3 is referred to as a "pseudo-layer" thickness because Y_2O_3 does not deposit as a smooth continuous layer, but as a dispersion of nanoparticles. As such, the reporting of the Y_2O_3 pseudo-layer thickness is the thickness of the layer if the deposition resulted in a smooth continuous layer. The determination of the layer or pseudo-layer thickness was done by depositing approximately 300 nm thickY123 on $SrTiO_3$ and Y_2O_3 on YSZ, respectively, and measuring the resulting thickness using a P-15 Tencor profilometer with $\pm$2 nm accuracy, and then calculating the corresponding deposition rate. The overall film thickness was measured upon completion of testing and compared to expected values to insure consistency.

The Y123 and Y_2O_3 targets were commercially manufactured and had purities of 99.999% and

99.99%, respectively, as reported by the manufacturer. Sample sizes were 3.2 mm × 3.2 mm × 0.5 mm for VSM measurements, and 5 mm × 10 mm × 0.5 mm for transport current measurements. The substrates were ultrasonically cleaned with acetone and isopropyl alcohol before being adhered to the heater with colloidal Ag paint. The chamber was pumped down to a base pressure of $<10^{-6}$ Torr. The depositions were done at 780 °C (±5 °C) in a flowing 300 mtorr O_2 (99.999% purity) pressure. The heater temperature was cross-checked with an Ircon infrared thermometer (Maxline series M-type). After the deposition was complete, the samples were cooled to 500 °C and held at that temperature under 800 mtorr O_2 pressure for a 30 min oxygenation.

Magnetic critical current density (J_{cm}) measurements were done with a vibrating sample magnetometer (VSM) at 70 and 77 K with field strengths up to 9 T ($H \| c$-axis). The J_{cm} of the samples was calculated using a simplified Bean model, $J_{cm} = 15\Delta M/R$, where ΔM is the magnetization/volume from 2 legs of the M–H loop and R is the radius of the induced circulating currents (cgs units), which was taken as one half of the average length of the four sides of the square samples. The film thickness were measured in three different positions in order to calculate the average film volume. The superconducting transition temperature (T_c) was measured using an ac susceptibility technique [16].

The contacts on the transport critical current density (J_{ct}) samples were made by dc magnetron sputtering a 3 μm thick layer of Ag onto the samples unmasked ends. The samples were then annealed at 550 °C for 30 min and re-oxygenated at 500 °C for 2 h in a sealed tube furnace at 1 atm O_2 (99.99% purity) flowing at 0.1 l/min. Bridges on the J_{ct} samples were between 0.6 and 0.75 mm wide and 3 mm long. The bridges were made by masking the samples with laser cut polyimide film (low static, 3M) and etching with a 2% nitric acid solution. Transport critical current measurements (self-field) were made in liquid nitrogen at 77 K with a 4-probe method using a 1 μV/cm criterion. The bridge width and film thickness were measured using the profilometer described previously.

3. Results and discussion

With the addition of Y_2O_3 layers to YBCO, the T_c was observed to be reduced in a fairly linear relationship with increasing Y_2O_3 pseudo-layer thickness, as shown in Fig. 1 for a constant Y123 layer thickness. The T_c was lowered by approximately 0.25 K for every 0.1 nm increase of the Y_2O_3 pseudo-layer thickness. The precise cause of the decrease is unclear; however, it may result from an increase of intrinsic strain on the YBCO layer thickness with increasing volume fraction addition of Y_2O_3. A similar decrease of $T_c \sim 2$–4 K was observed in (Y211/Y123) × N multilayer films with Y211 nanoparticle additions [3].

The SEM images in Fig. 2(a)–(c) indicate there is good nanoparticle formation on the composite film surface, varying as a function of the Y_2O_3 pseudo-layer thickness. The white-image nanoparticles are assumed to be Y_2O_3 or similar phase, as the comparative insulating nature of the particles causes the increased secondary emission and appears relatively brighter in the images in contrast to the YBCO base layers. It can be seen in the Fig. 2(a)–(c) that the nanoparticle size is only slightly increased as the Y_2O_3 thickness is increased; the 0.2 nm pseudo-layer gives average particle diameter (D_{avg}) ~ 11.2 nm/particle and the 1.4 nm pseudo-layer gives $D_{avg} \sim 12.9$ nm/particle. However, as the thickness of the Y_2O_3

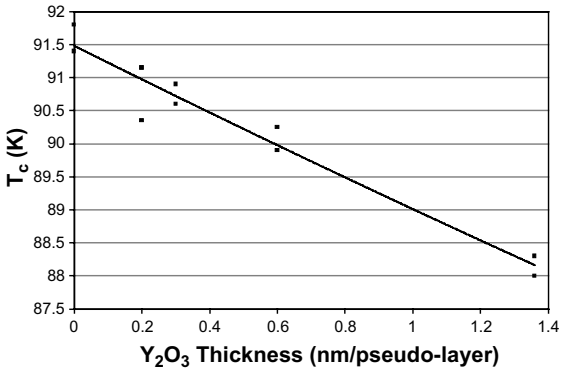

Fig. 1. Critical temperature as a function of Y_2O_3 'pseudo-layer' thickness of Y_2O_3/Y123 multilayer films; Y123 = 10 nm/layer and total film thickness ~0.3 μm. The T_c was reduced about 0.25 K for each 0.1 nm increase in Y_2O_3 thickness.

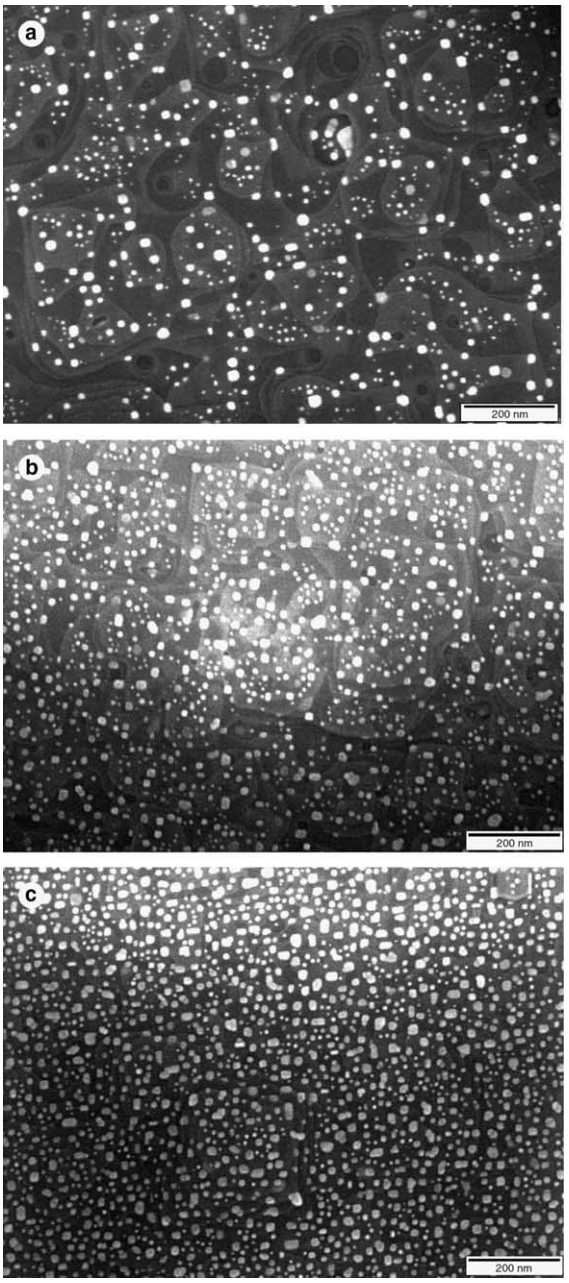

Fig. 2. SEM images of Y_2O_3/Y123 multilayer film surfaces for varying Y_2O_3 pseudo-layer thickness: (a) 0.2 nm Y_2O_3 pseudo-layer ($\sim 0.8 \times 10^{11}$ particles/cm^2), (b) 0.48 nm Y_2O_3 pseudo-layer ($\sim 1.25 \times 10^{11}$ particles/cm^2), (c) 1.4 nm Y_2O_3 pseudo-layer ($\sim 1.6 \times 10^{11}$ particles/cm^2). Note preferential deposition of nanoparticles on Y123 plateau edges and corners, and little increase in particle diameters. Magnification 100 k×.

pseudo-layer was increased, the number density of Y_2O_3 particles increased significantly from 8×10^{10} to 1.6×10^{11} particles/cm^2. The increase of particle size and number density is consistent with the increase of deposited material. While nanoparticles were observed on the film surfaces, the structure of an embedded Y_2O_3 nanoparticulate layer is unclear since TEM imaging of the samples is not yet complete. Even so, it is believed that the structure will be similar to that seen in the Y211/Y123 composite multilayer films [3]. In general, a thicker pseudo-layer results in a higher density of nanoparticles with only a slight increase in nanoparticle size. As such, the correlation between the reduction in T_c versus pseudo-layer thickness may suggest that strain in the Y123 film is a significant contributing factor.

Typical T_c transitions of the composite Y_2O_3/Y123 thin films as measured by ac susceptibility are plotted and compared to pure Y123 films in Fig. 3. The spread of the $4\pi\chi$ plots in different magnetic fields for the composite film is larger than that of the plain Y123 film, but not significantly, indicating good film quality [17,18]. J_{ct}s of 3–5 MA/cm^2 (77 K, self-field) were consistently measured with the composite films containing $\leqslant 0.6$ nm Y_2O_3 pseudo-layer thickness (Fig. 4), which are basically the same J_{ct} values obtained

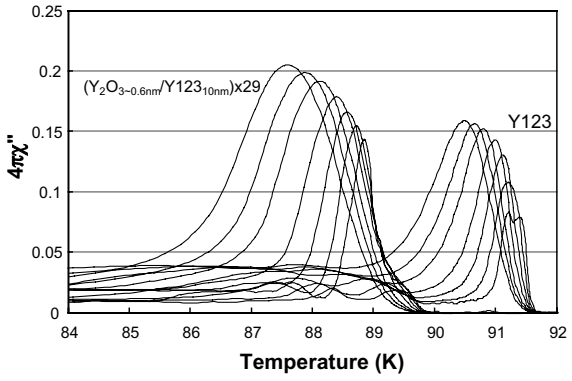

Fig. 3. AC susceptibility plots of Y_2O_3/Y123 multilayer and pure Y123 thin films on $\langle 100 \rangle SrTiO_3$ substrates. Transitions are plotted for each film for 0.025, 0.1, 0.25, 0.5, 1.0, 1.5 to 2.2 Oe field strengths, plotted right to left decreasing in temperature with increasing field strength. The multilayer films showed a slight increase in the superconducting transition widths for the field strengths tested.

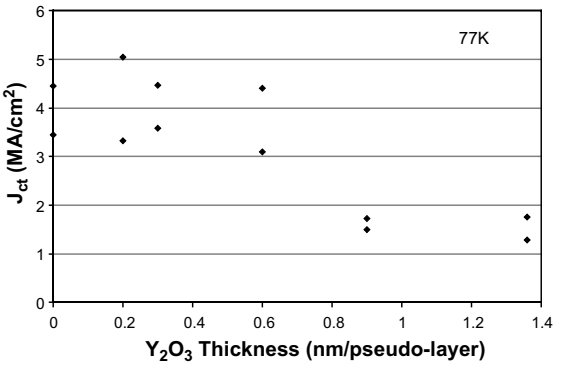

Fig. 4. Transport critical currents (77 K, self-field) as a function of Y_2O_3 pseudo-layer thickness, for constant Y123 layer thickness ~10 nm.

for YBCO only films (Y_2O_3 thickness = 0 in Fig. 4). This indicates that the limited Y_2O_3 addition does not have detrimental effect on the critical current flows for self-field current measurements. However, as the Y_2O_3 pseudo-layer thickness was increased >0.6 nm, a significant decrease of critical currents was observed. The inclusion of 0.9 nm Y_2O_3 pseudo-layers in the composite film resulted in J_{ct} (77 K, self-field) being reduced to ~(1.3–2.6) MA/cm^2. The exact cause of the decrease is unclear, and there is no evidence yet of any structural relationship between the changes in Y123 layer thickness and J_{ct} when the Y_2O_3 pseudo-layer thickness is kept constant. Although not shown here, a similar range of J_{ct} (77 K, self-field) ~3–5 MA/cm^2 was measured for multiple films where Y_2O_3 was <0.6 nm, even though the Y123 layer thickness was varied from 7 nm to 50 nm.

Magnetic J_c measurements (J_{cm}) at 77 K of the composite multilayered films with a Y_2O_3 pseudo-layer thickness of 0.3 nm or less showed some improvement compared to Y123 films at field strengths above 4 T (Fig. 5), but not significant differences for $H < 4$ T. Films with a large Y_2O_3 layer thickness of 1.36 nm showed markedly poor $J_{cm}(H)$ compared to Y123 films. It is speculated that the Y_2O_3 layer is becoming too complete (Fig. 2) and not allowing effective vortex formation to extend throughout the structure for effective pinning.

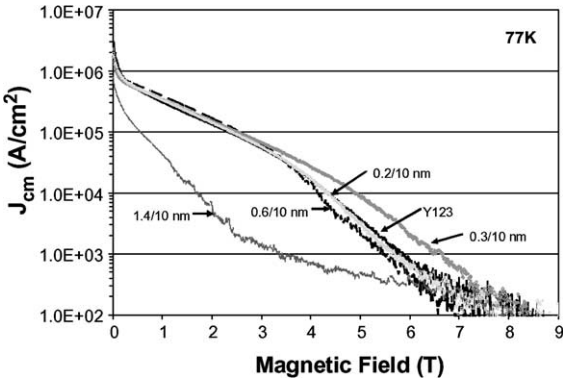

Fig. 5. J_{cm} measurements at 77 K of Y_2O_3/Y123 multilayer films with different Y_2O_3 pseudo-layer thicknesses and constant Y123 thickness ~10 nm. A slight improvement over Y123 only films was seen in films with approximately 0.3 nm Y_2O_3 pseudo-layer thickness. Multilayer labels: 0.3/10 nm = 0.3 nm Y_2O_3 pseudo-layer thickness/10 nm Y123 pseudo-layer thickness.

It was found that improvement of J_{cm} over the plain Y123 values was enhanced with the 0.3 nm Y_2O_3 pseudo-layers when the number of Y_2O_3 pseudo-layers was reduced and the Y123 layer of the composite film was increased. The increase can be seen in Fig. 6, with improvement as much as 6 times especially for field strengths of 3.5–7 T. All depositions were made to result in equal composite film total thickness. The average thickness was found to be 0.314 ± 0.015 μm via profilometry measurements.

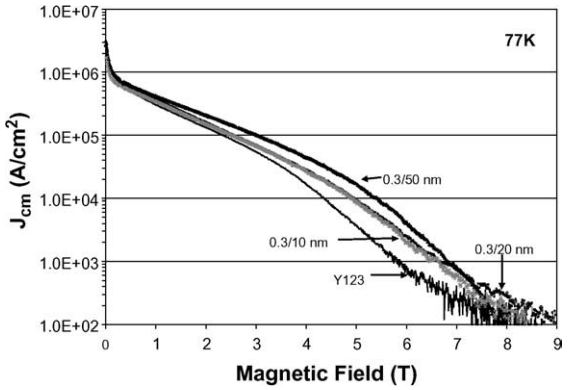

Fig. 6. J_{cm} measurements at 77 K for Y_2O_3/Y123 multilayer films with increased Y123 layer thickness, and constant Y_2O_3 pseudo-layer thickness ~0.3 nm. The reduction in number of layers and increase of the Y123 thickness showed good improvement of J_c for the range of field strengths tested. Labeling structure same as Fig. 5.

J_{cm} measurements at 70 K demonstrated that magnetic flux pinning was more pronounced at the lower temperature, as shown in Figs. 7 and 8 for the films also measured at 77 K. In Fig. 7, the multi-layer films with $\leqslant$0.6 nm Y_2O_3 pseudo-layer thickness improved the pinning at fields above 4.5 T. The film with 0.6 nm Y_2O_3 thickness showed comparatively enhanced pinning at 70 K as compared to 77 K. At 70 K the relative current density was increased, and a stronger effect was seen from the higher Y_2O_3 particle number density. The J_{cm} values (at 70 K) in Fig. 8 showed an increase at higher fields similar to that seen at 77 K, when the Y123 layer thickness was increased.

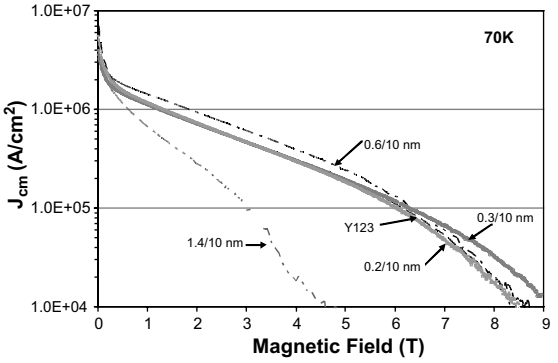

Fig. 7. J_{cm} measurements at 70 K of multilayer films with various Y_2O_3 pseudo-layer thicknesses for films measured in Fig. 5. The films with $Y_2O_3 \leqslant 0.6$ nm pseudo-layer thickness showed improvement at the reduced temperature.

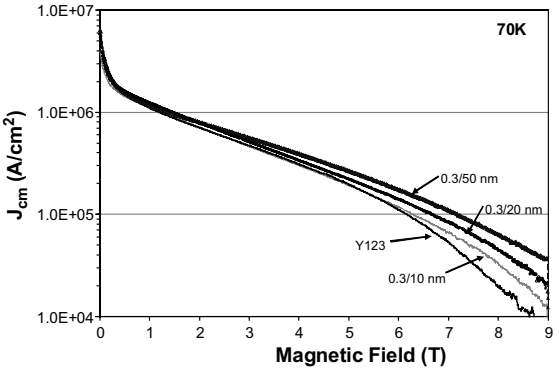

Fig. 8. J_{cm} measurements at 70 K for multilayer films with increased Y123 layer thickness from Fig. 6. The improvements were similar to those seen at 77 K for the range of field strengths tested.

A J_{cm} comparison of Y_2O_3/Y123 multilayer films toY211/Y123 multilayer films with equivalent Y123 layer thicknesses are shown in Figs. 9 and 10. In both Figs. 9 and 10, the J_{cm} measurements of a Y123 film on $SrTiO_3$ was added for comparison. The $J_{cm}(H)$ curve for Y123 chosen was representative of several measurements and similar curves on both $LaAlO_3$ and $SrTiO_3$. Small differences of the $J_{cm}(H)$ curves for Y123 were

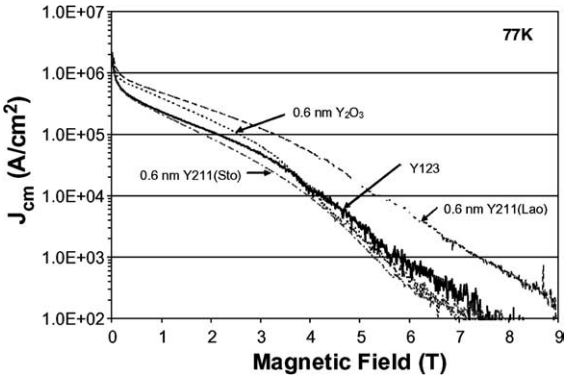

Fig. 9. J_{cm} comparison of Y_2O_3/Y123 multilayer film with 0.6 nm Y_2O_3 pseudo-layer thickness and Y211/Y123 multilayer films with 0.6 nm Y211 pseudo-layer thickness, each with approximately equal Y123 layer thickness. The plot shows the normal deviation seen in multilayer film depositions, and improvement of (Y_2O_3/Y123) compared to (Y211/Y123) multilayer films for fields <4 T.

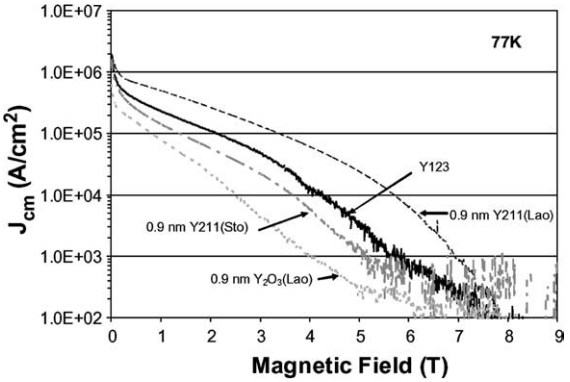

Fig. 10. J_{cm} comparison of Y_2O_3/Y123 multilayer film with 0.9 nm Y_2O_3 pseudo-layer thickness and Y211/Y123 multilayer films with 0.9 nm Y211 pseudo-layer thickness, each with approximately equal Y123 layer thickness. The plot shows the deterioration of film properties due to the increased Y_2O_3 pseudo-layer thickness.

observed to vary primarily based on initial differences of self-field J_{ct} values; the trends for $J_{cm}(H)$ for Y123 showed little variations otherwise. From Fig. 9, it can be seen that the Y_2O_3/Y123 multilayer performs better than Y211/Y123 multi-layer film on the STO substrate, but not as well as the Y211/Y123 multilayer on the LAO substrate. This combined with differences between the Y211 and Y_2O_3 composite films' behavior, especially at fields <4 T, suggesting differences in pinning resulting from how the Y_2O_3 particulates form, specifically the density of nanoparticles and the nanoparticulate size [19].

The Y_2O_3/Y123 multilayer films with more than 0.6 nm Y_2O_3 pseudo-layer thickness showed drastic deterioration of $J_{cm}(H)$ over the entire range of applied magnetic fields tested (0–9 T). As an example in Fig. 10, a comparison of composite film with a 0.9 nm Y_2O_3 pseudo-layer thickness versus a composite film with a 0.9 nm Y211 pseudo-layer thickness is shown. The deterioration of the $J_{cm}(H)$ properties at this Y_2O_3 pseudo-layer thickness are clearly evident. The deterioration is speculated to result from differences of nanoparticle height/width ratio and overall surface coverage between the Y_2O_3 and Y211 insulating layer [19]. The Y_2O_3 nanoparticles are predicted to be thinner and have larger diameter because of a much smaller lattice mismatch with YBCO (0.6% compared to ~2–7% for Y211), and therefore the Y_2O_3 pseudo-layer would have larger coverage for a same 'pseudo-layer' thickness. A critical threshold for 'pseudo-layer' thickness was observed for both Y_2O_3 and Y211 particulate interlayers, above which the self-field and $J_{cm}(H)$ properties began to degrade significantly (Figs. 5 and 7). The 'pseudo-layer' thickness threshold for Y211 was previously found to be higher, about 2.0 nm [3,4] compared to about 0.7 nm for Y_2O_3.

4. Conclusion

The use of Y_2O_3 nanoparticulates showed potential as flux pinning centers in YBCO thin films. The results were slightly better than those by previous researchers utilizing different techniques [4–6]. As observed on film surfaces, the size of the Y_2O_3 nanoparticulates remained relatively steady while the number density could be adjusted by increasing the number of laser pulses on the Y_2O_3 target. The nanoparticulate additions caused only minimal reductions (1.8 K for 0.6 nm pseudo-layer) in the critical temperature. Even so, it was found that an Y_2O_3 pseudo-layer thickness of greater than 0.6 nm could decrease the self-field (J_{ct}) and magnetic critical currents (J_{cm}) for the range of applied magnetic fields (0–9) T. The reduction of the number of layers and increase of the Y123 layer thickness exhibited increased magnetic field properties when an optimized Y_2O_3 pseudo-layer thickness was used. Even though the Y211/Y123 composite films from a previous work [3,4] in general outperformed the Y_2O_3/Y123 composite films, further optimization of the Y_2O_3/Y123 structure is possible by considering variations of Y_2O_3 and Y123 layer thickness along with other deposition parameters.

Acknowledgments

The authors would like to thank J.M. Evans, J. Kell, N. Yust, and Srinivas Sathiraju in the Propulsion Directorate of the Air Force Research Laboratory for their help in data acquisition and measurements.

References

[1] D. Larbalestier, A. Gurevich, M. Feldman, A. Polyanskii, Nature 414 (2001) 368.
[2] P.N. Barnes, G.L. Rhoads, J.C. Tolliver, M.D. Sumption, K.W. Schmaeman, IEEE Trans. Magn. 41 (2005) 268.
[3] T. Haugan, P.N. Barnes, I. Maartense, C.B. Cobb, E.J. Lee, M. Sumption, J. Mater. Res. 19 (2003) 2618.
[4] T.J. Haugan, P.N. Barnes, R. Wheeler, F. Meisenkothen, M. Sumption, Nature 430 (2004) 867.
[5] P.R. Broussard, V.C. Cestone, L.H. Allen, IEEE Trans. Appl. Supercond. 5 (1995) 1222.
[6] P. Lu, Y.Q. Li, J. Zhao, C.S. Chern, B. Gallois, P. Norris, B. Kear, F. Cosandey, Appl. Phys. Lett. 60 (1992) 1265.
[7] P.R. Broussard, V.C. Cestone, L.H. Allen, J. Appl. Phys. 77 (1995) 252.
[8] M. Murakami, S. Gotoh, H. Fujimoto, K. Yamaguchi, N. Koshizuka, S. Tanaka, Supercond. Sci. Technol. 4 (1991) S43.
[9] B. Ni, M. Kiuchi, E.S. Otabe, IEEE Trans. Appl. Supercond. 13 (2003) 3695.

[10] N. Hari Babu, E. Sudhakar Reddy, D.A. Cardwell, A.M. Campbell, Supercond. Sci. Technol. 16 (2003) L44.
[11] D.B. Jan, J.Y. Coulter, M.E. Hawley, L.N. Bulaevski, M.P. Maley, Q.X. Jia, B.B. Maranville, F. Hellman, X.Q. Pan, Appl. Phys. Lett. 82 (2003) 778.
[12] G. Kastner, D. Hesse, R. Scholz, H. Koch, F. Ludwig, M. Lorenz, H. Kittel, Physica C 243 (1995) 281.
[13] J.L. MacManus-Driscoll, S.R. Foltyn, Q.X. Jia, H. Wang, A. Serquis, L. Civale, B. Maiorov, M.E. Hawley, M.P. Maley, D.E. Peterson, Nature Mater. 3 (2004) 439.
[14] P.N. Barnes, R.M. Nekkanti, T.J. Haugan, T.A. Campbell, N.A. Yust, J.M. Evans, Supercond. Sci. Technol. 17 (2004) 957.
[15] T. Haugan, P.N. Barnes, L. Brunke, I. Maartense, J. Murphy, Physica C 397 (2003) 47.
[16] J.R. Thompson, L. Krusin-Elbaum, Y.C. Kim, D.K. Christen, A.D. Marwick, R. Wheeler, C. Li, S. Patel, D.T. Shaw, P. Lisowski, J. Ullmann, IEEE Trans. Appl. Supercond. 5 (1995) 1876.
[17] I. Maartense, A.K. Sarkar, G. Kozlowski, Physica C 181 (1991) 25.
[18] P.N. Barnes, I. Maartense, T.L. Peterson, T.J. Haugan, A.L. Westerfield, L.B. Brunke, S. Sathiraju, J.C. Tolliver, Mat. Res. Soc. Symp. Proc., EXS-3, pp. EE6.4.1-3, 2004.
[19] P.N. Barnes, T.J. Haugan, C.V. Varanasi, T.A. Campbell, Appl. Phys. Lett. 85 (2004) 4088.